A Generalized Approach to the Modification of Solid Surfaces

Du Yeol Ryu,[1] Kyusoon Shin,[1] Eric Drockenmuller,[2] Craig J. Hawker,[2]* Thomas P. Russell[1]*

Interfacial interactions underpin phenomena ranging from adhesion to surface wetting. Here, we describe a simple, rapid, and robust approach to modifying solid surfaces, based on an ultrathin cross-linkable film of a random copolymer, which does not rely on specific surface chemistries. Specifically, thin films of benzocyclobutene-functionalized random copolymers of styrene and methyl methacrylate were spin coated or transferred, then thermally cross-linked on a wide variety of metal, metal oxide, semiconductor, and polymeric surfaces, producing a coating with a controlled thickness and well-defined surface energy. The process described can be easily implemented and adapted to other systems.

Controlling surface energies affords precise control over the surface and interfacial properties of a material, ranging from wetting to adhesion and, more recently, the orientation of nanoscopic structure in thin polymer films. Controlled interfacial interactions also find applications in synthetic (*1*–*6*) and biological systems (*7*) as surface-responsive materials (*8*). As a result of this rich array of applications, much attention has been placed on strategies to precisely tune interfacial and surface interactions of materials. Traditional approaches, however, rely on the use of surface-specific chemistries, such as aggressive ion beam techniques, self-assembly processes, or the chemical attachment of long-chain molecules to a surface. A notable drawback to these approaches is that they are not general and cannot be applied to a wide range of surfaces or substrates. For example, chlorosilane chemistries can easily be used on an oxide surface but cannot be used to modify the surface of gold or polymer films. Similarly, controlling the chemical composition with end-functionalized random copolymers allows exquisite control over surface energy, but the attachment of the chain requires time to have chain ends diffuse to the surface and very specific interactions and/or chemistries of the end group with the substrate (*1*). To date, there is no general approach to control interfacial and/or surface interactions. Here, we present a simple yet extremely versatile strategy, based on the cross-linking of ultrathin random copolymer films, for controlling and modifying interfacial and surface interactions.

This strategy takes advantage of the inherent versatility of random copolymers, which allows the surface energy or surface characteristics to be tuned by changing the chemical composition of the random copolymer. However, rather than relying on an inefficient and slow grafting procedure in which the chain end of the random copolymer diffuses to the surface and undergoes a very specific reaction with the surface, we used random copolymers containing a cross-linking group placed along the backbone. Using a simple, highly efficient cross-linking reaction, we obtained an insoluble, ultrathin film of the random copolymer that is more robust than an anchored random copolymer chain and, moreover, is independent of surface chemistry.

We studied random copolymers of styrene (S) and methyl methacrylate (MMA) with 2% reactive benzocyclobutene (BCB) functionality randomly incorporated along the backbone as an example. After spin coating, the BCB units in the BCB-functionalized polystyrene-*r*-poly(methyl methacrylate) copolymer [P(S-*r*-BCB-*r*-MMA)] can be thermally cross-linked to give a random copolymer network in which the thickness of the film is controlled by the concentration of the random copolymer solution spin coated onto the surface. The strength of the interfacial interactions can be changed by controlling the relative composition of S and MMA in the copolymer. In addition, the degree of cross-linking can be altered by changing the number of BCB units incorporated into the copolymer. The cross-linked film is insoluble and compatible with further processing. Removing the requirement of chemical attachment to the underlying substrate allows these cross-linked ultrathin films to be placed on most surfaces that can be coated. Even without chemical bonding to the surface, adhesive failure of the thin films was not observed (*9*) and the random copolymer architecture affords tremendous flexibility in circumventing this. In the case of PS and PMMA, previous studies have shown that a random copolymer containing 58% S that is end-anchored to the substrate produces a surface on which the interfacial interactions are balanced (*1*). Because BCB is chemically similar to S, the proportion of S/BCB/MMA in the copolymer used was 56/2/42. The random copolymer was prepared by nitroxide-mediated, living free radical polymerization (Scheme 1). To ensure sufficient cross-link density, molecular weights of between 20,000 and 100,000 were used with a typical sample having a number average molecular weight of 35,000 and a polydispersity of 1.18, which corresponds to an average of seven BCB units per chain. The polystyrene–poly(methyl methacrylate) block copolymer (PS-*b*-PMMA) used in these studies was prepared by anionic polymerization and had a weight average molecular weight of 88,000, a polydispersity of 1.03, and a 0.72 volume fraction of PS (*9*). In the bulk, the morphology consists of hexagonally packed cylindrical microdomains of PMMA in a PS matrix with a lattice spacing L_o = 34.1 nm. Thin films of PS-*b*-PMMA for which the micro-

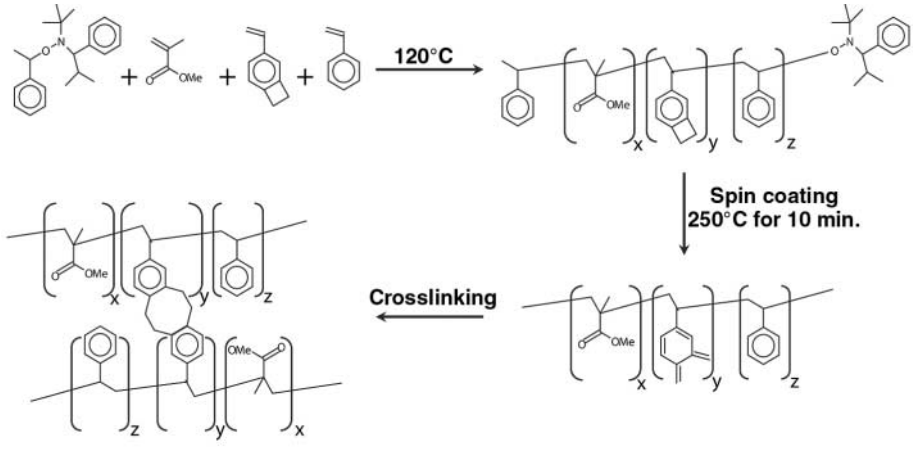

Scheme 1. Synthesis and primary cross-linking reaction of the P(S-*r*-BCB-*r*-MMA), which has a composition of 56/2/42 for PS/BCB/PMMA.

[1]Polymer Science and Engineering Department, University of Massachusetts, Amherst, MA 01003, USA. [2]IBM Almaden Research Center, 650 Harry Road, San Jose, CA 95120, USA.

*To whom correspondence should be addressed. E-mail: hawker@mrl.ucsb.edu (C.J.H.); russell@mail.pse.umass.edu (T.P.R.)

domain orientation can be controlled have tremendous potential as templates and scaffolds for the fabrication of nanoscopic materials (*10*–*16*).

A 0.3–weight percent (wt %) solution of P(S-*r*-BCB-*r*-MMA) in toluene was spin coated onto a silicon wafer to yield films ~11.1 nm thick. The coated substrates were heated under a nitrogen atmosphere to either 200° or 250°C [well above the glass transition temperatures of PS (100°C) and PMMA (115°C)] for different periods of time to investigate the cross-linking of the random copolymer. Subsequently, the films were thoroughly rinsed with toluene to remove material that was not cross-linked and the thickness of the insoluble cross-linked random copolymer remaining on the substrate surface was measured by ellipsometry (Fig. 1). The thickness of the film increased as time increased, and after 4 hours at 200°C or 10 min at 250°C, the film thickness reached a constant value of 10.4 nm. The final value of 10.4 nm is ~6% thinner than the initial film thickness of 11.1 nm, reflecting the volume shrinkage associated with cross-linking. As the data in Fig. 1 show, the rate of cross-linking decreases as temperature decreases, and, from independent measurements, ~150°C sets an effective lower limit on the efficiency of the BCB cross-linking. This lower temperature limit does prevent us from coating crystallizable polymers with low melting temperatures. Although it was possible to coat these materials, volume contractions and marked changes to the surface topography that occur during crystallization damaged the coating.

To demonstrate the effectiveness of these cross-linked random copolymer mats in controlling surface energy, thin films (~10 nm) of PS and PMMA homopolymers were spin coated onto Si substrates coated with cross-linked P(S-*r*-BCB-*r*-MMA) films (10 min at 250°C) (Fig. 1). The homopolymer films were then heated to 170°C for 3 days, allowing the homopolymer films to dewet. The shapes of the edges of the dewetted PS and PMMA films were determined from the height profiles with scanning force microscopy. From the shape, the contact angles of the PS and PMMA on the P(S-*r*-BCB-*r*-MMA) were determined and are plotted in Fig. 2 as a function of the thickness of the P(S-*r*-BCB-*r*-MMA) on the surface. In the case of PS, the contact angle is initially ~13°, decreases to 9.0° as the thickness of the P(S-*r*-BCB-*r*-MMA) film increases to ~5 nm, and then remains constant for thicker P(S-*r*-BCB-*r*-MMA) coatings. PMMA, on the other hand, has a contact angle of ~5° that increases to 10.1° when the P(S-*r*-BCB-*r*-MMA) coating is ~5 nm, and remains constant for thicker coatings of the random copolymer. Thus, for P(S-*r*-BCB-*r*-MMA) coatings, 5 nm or thicker, the contact angles for PS and PMMA are essentially the same. The changes in the contact angles for the PS and PMMA can be understood when one considers the increasing number of P(S-*r*-BCB-*r*-MMA) cross-links, the increasing thickness of the random copolymer film, and the decreasing penetration of the homopolymer to the underlying oxide layer of the substrate. The constant contact angles obtained for PS and PMMA on random copolymer films thicker than 5 nm (cross-linked for 10 min at 250°C) can be used to evaluate the interfacial energies from Young's equation:

$$\gamma_{if} = \gamma_f - \gamma_i \cos\theta_{if} \quad (1)$$

where γ_i and γ_f are the surface tensions of the homopolymer and the random copolymer, respectively, and θ_{if} is the contact angle of the homopolymer on the cross-linked random copolymer mat. From previous studies (*1*), $\gamma_S = 29.9$ erg/cm^2 for PS, $\gamma_M = 30.02$ erg/cm^2 for PMMA, and $\gamma_f = 29.95$ erg/cm^2 for a neutral random copolymer brush that has 58% of S. From the contact angles of 9.0° and 10.1° for PS and PMMA, respectively, $\gamma_{Sf} = 0.415$ erg/cm^2 and $\gamma_{Mf} = 0.397$ erg/cm^2. These are the same to within experimental error and, consequently, the interfacial interactions are balanced.

Films of cross-linked P(S-*r*-BCB-*r*-MMA), 7 nm in thickness after heating to 250°C for 10 min under nitrogen, were prepared on a variety of substrates, including metals (Au and Al), semiconductors (Si, SiOx, and Si_3N_4), and polymers [Kapton (aromatic polyimide) and polyethylene terephthalate (PET)]. These substrates present a wide range of interfacial interactions and chemistries that are not compatible with any one functionality. Notably, Au surfaces are difficult to modify in a robust manner with thiol monolayers, because typical annealing temperatures of the block copolymers are ~170°C, which is much greater than the dissociation temperature of the Au-thiol bond. Shown in Fig. 3, A and B, are water droplets on a silicon wafer and Au substrate, respectively, coated with 7-nm layer of cross-linked P(S-*r*-BCB-*r*-MMA). The contact angles are 76.2° and 76.1°, respectively. Without the random copolymer layer, the contact angles are 17.4° for SiO_2 (Fig. 3C) and 63.4° for Au (Fig. 3D). As shown, the surface energies of the hydrophilic (silicon oxide) and hydrophobic (Au) surfaces have been changed and are identical.

A P(S-*b*-MMA) diblock copolymer film, ~33 nm or L_o in thickness, was spin coated onto Au-patterned Si substrates, prepared by thermal evaporation with a mask (a Cr adhesion layer was needed to adhere the Au to the substrate), without (Fig. 3E) or with (Fig. 3F) a 7-nm layer of cross-linked P(S-*r*-BCB-*r*-MMA), and annealed for 24 hours under vacuum at 170°C. Shown in Fig. 3, G to J, are scanning force microscopy phase images of the block copolymer film on the bare Au (Fig. 3G) and silicon oxide–coated (Fig. 3I) portions of the substrates and the corresponding sections (Fig. 3, H and J) coated with a 7-nm-thick layer of cross-linked P(S-*r*-BCB-*r*-MMA). The surfaces coated with P(S-*r*-BCB-*r*-MMA), on which the interfacial interactions are balanced (*1*, *17*), produce films in which the cylindrical microdomains are oriented normal to the surface, regardless of the underlying substrate. However, on the bare Au surface poor control over the microdomain orientation was achieved (Fig. 3G), and on the silicon oxide surface the microdomains orient parallel to the surface (Fig. 3I) and show the classic island and hole topography. In agreement with the PS and

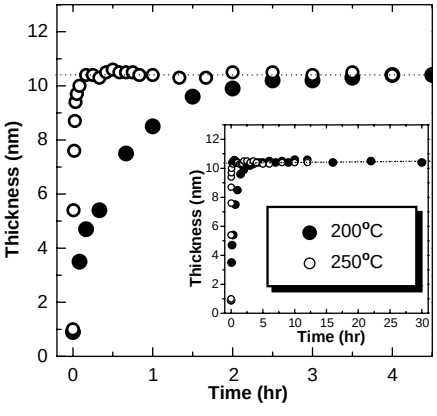

Fig. 1. The thickness of the P(S-*r*-BCB-*r*-MMA) film as a function of the reaction time at 200° and 250°C after rinsing with a good solvent.

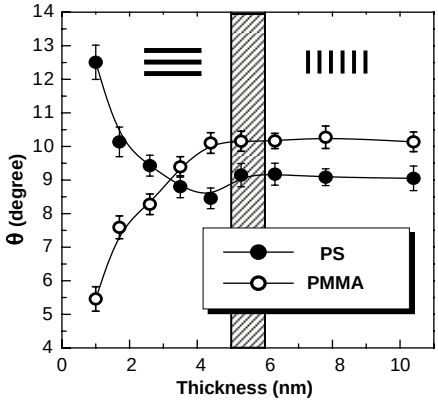

Fig. 2. Contact angles for PS and PMMA as a function of P(S-*r*-BCB-*r*-MMA) film thickness after annealing at 250°C for 10 min, when the copolymer is fully cross-linked and there is no change in film thickness upon rinsing with a good solvent. Homopolymer films (~10 nm thick) were spin coated onto the P(S-*r*-BCB-*r*-MMA) modified substrates and annealed at 170°C for 3 days. For clarity, a shaded region at 5.5 ± 0.5 nm marks the P(S-*r*-BCB-*r*-MMA) thickness where a change in the microdomain orientation (from parallel to perpendicular) was observed for P(S-*b*-MMA) copolymer. Error bars show mean ± SD.

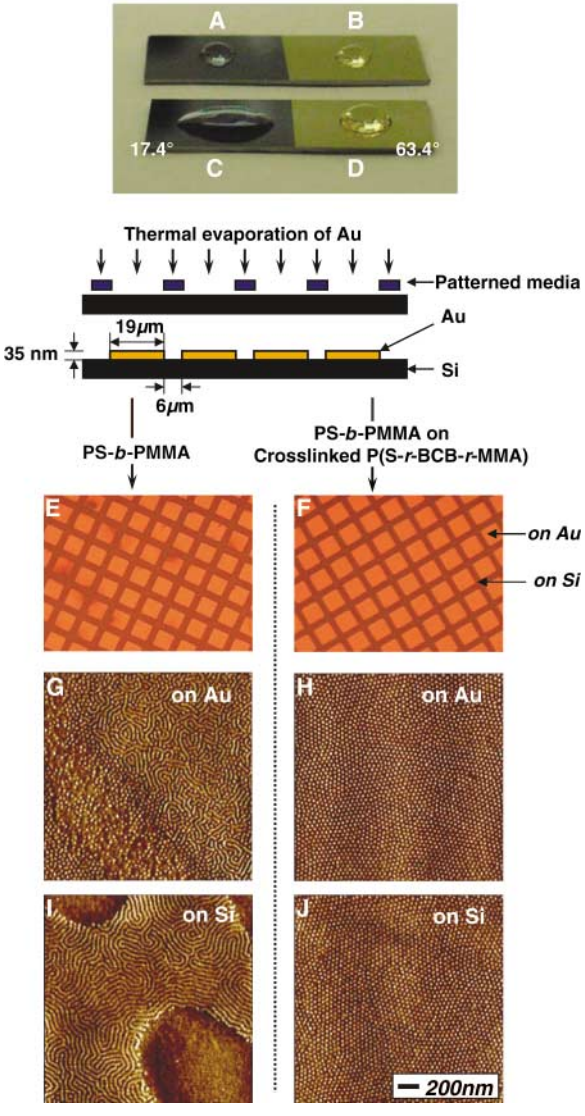

Fig. 3. Water droplets on the Si (**A**) and Au (**B**) substrates coated with a 7-nm-thick cross-linked film of P(S-*r*-BCB-*r*-MMA) and on bare Si (**C**) and Au (**D**) substrates without the copolymer. A P(S-*b*-MMA) copolymer spin coated and annealed for 1 day at 170°C onto the Au-patterned Si substrate prepared by thermal evaporation with a patterned mask without (**E**) or with (**F**) cross-linked random copolymer mat. Scanning force microscopy phase images of a P(S-*b*-MMA) copolymer on the bare Au (**G**) and Si (**I**) substrates and on the Au (**H**) and Si (**J**) substrates with cross-linked random copolymer mat. Block copolymer films are ~33 nm (or ~1 L_o) thick and the *z* range of phase images is between ~6° and ~10°.

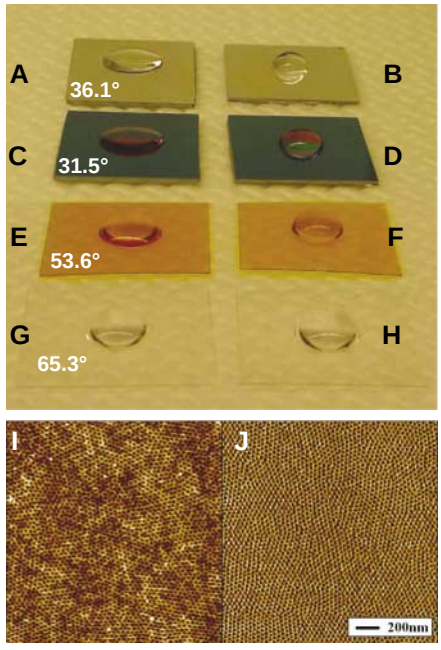

Fig. 4. Water droplets on bare Al (**A**), Si_3N_4 (**C**), Kapton (**E**), and PET (**G**) substrates. The contact angles range from 31.5° to 65.3° depending on the substrate. Water droplets on each substrate coated with 7-nm layer of cross-linked P(S-*r*-BCB-*r*-MMA), however, are the same 76° ± 0.3° (**B**, **D**, **F**, and **H**). Scanning force microscopy height (**I**) and phase (**J**) images of a ~33-nm-thick film of P(S-*b*-MMA) copolymer prepared on substrates coated with a film of cross-linked random copolymer mat regardless of the underlying substrate. PMMA was selectively removed by exposing the film to ultraviolet radiation and rinsing with acetic acid as a good solvent for PMMA. This nanoporous PS film constitutes a template or scaffold for the fabrication of nanostructured materials.

PMMA dewetting studies, a layer of P(S-*r*-BCB-*r*-MMA) at least 5 nm in thickness was required to control the microdomain orientation (indicated by the vertical shaded region in Fig. 2). In addition, the thin film of cross-linked P(S-*r*-BCB-*r*-MMA) protects the Cr adhesion layer from oxidation. Many defects are seen in the untreated patterned surface (compare Fig. 3, E and F).

The versatility of the cross-linked random copolymer mat approach is demonstrated in Fig. 4, which shows water droplets on bare Al (Fig. 4A), Si_3N_4 (Fig. 4C), Kapton (Fig. 4E), and PET (Fig. 4G) substrates. The contact angles range from 31.5° to 65.3° depending on the substrate. When these substrates are coated with a 7-nm layer of cross-linked P(S-*r*-BCB-*r*-MMA), however, all of the contact angles to within one standard deviation (±SD) are the same at 76° ± 0.3° (Fig. 4, B, D, F, and H). L_o thick films of P(S-*b*-MMA) spin coated onto each of the substrates coated with the 7-nm-thick cross-linked random copolymer mat showed an orientation of the cylindrical microdomains normal to the surface regardless of the underlying substrate. When we exposed these films to ultraviolet radiation, the PS was cross-linked and the PMMA was degraded; after rinsing with acetic acid, pores were produced (as evidenced by scanning electron microscopy) that extend from the film surface to the underlying substrate. In both the height (Fig. 4I) and phase images (Fig. 4J), cylindrical pores with 20-nm diameters are seen in the PS matrix (with a 34.1-nm spacing). Even though the random copolymer mat contains MMA, the integrity of the underlying random copolymer film is maintained by virtue of the cross-linking and the block copolymer template remains intact.

We have developed a method in which the interfacial interactions of a surface can be easily manipulated in a rapid, robust manner through the use of a thin, cross-linked random copolymer film. This technique does not require specific chemical reactions or interactions with the surface. Because the film is cross-linked, it is resistant to solvents and forms a robust coating on the surface. The effectiveness in controlling the interfacial interactions was demonstrated with thin diblock copolymer films on a wide range of substrates on which the orientation of the microdomains was demonstrated.

References and Notes

1. P. Mansky, Y. Liu, E. Huang, T. P. Russell, C. J. Hawker, *Science* **275**, 1458 (1997).
2. P. Wiltzius, A. Cumming, *Phys. Rev. Lett.* **66**, 3000 (1991).
3. G. Coulon, T. P. Russell, V. R. Deline, P. F. Green, *Macromolecules* **22**, 2581 (1989).
4. S. H. Anastasiadis, T. P. Russell, S. K. Satija, C. F. Majkrzak, *Phys. Rev. Lett.* **62**, 1852 (1989).
5. J. Genzer, K. Efimenko, *Science* **290**, 2130 (2000).
6. M. K. Chaudhury, G. M. Whitesides, *Science* **256**, 1539 (1992).
7. C. S. Chen, M. Mrksich, S. Huang, G. M. Whitesides, D. E. Ingber, *Science* **276**, 1425 (1997).
8. T. P. Russell, *Science* **297**, 964 (2002).
9. Materials and methods are available as supporting material on *Science* Online.
10. M. Park, C. Harrison, P. M. Chaikin, R. A. Register, D. H. Adamson, *Science* **276**, 1401 (1997).
11. A. Avgeropoulos *et al.*, *Chem. Mater.* **10**, 2109 (1998).
12. T. Thurn-Albrecht *et al.*, *Science* **290**, 2126 (2000).
13. T. Thurn-Albrecht *et al.*, *Adv. Mat.* **12**, 787 (2000).
14. C. T. Black *et al.*, *Appl. Phys. Lett.* **79**, 409 (2001).

15. P. Mansky, C. K. Harrison, P. M. Chaikin, R. A. Register, N. Yao, *Appl. Phys. Lett.* **68**, 2586 (1996).
16. K. Shin *et al.*, *Nano Lett.* **2**, 933 (2002).
17. E. Huang, L. Rockford, T. P. Russell, C. J. Hawker, *Nature* **395**, 757 (1998).
18. This work was supported by NSF Grant Opportunities for Academic Liaison with Industry award (DMI-0217816), the U.S. Department of Energy under contract DE-FG03-88ER45375 and the Materials Research Science and Engineering Centers at the University of Massachusetts (DMR-0213695) and Santa Barbara (DMR-0080034). D.Y.R. thanks the support by the Postdoctoral Fellowship program of Korea Science and Engineering Foundation in Korea. We thank C. Silvas of Dow Chemical for providing the brominated BCB.

Supporting Online Material
www.sciencemag.org/cgi/content/full/308/5719/236/DC1
Materials and Methods
Fig. S1

21 October 2004; accepted 22 February 2005
10.1126/science.1106604

Estimating Duration and Intensity of Neoproterozoic Snowball Glaciations from Ir Anomalies

Bernd Bodiselitsch,[1] Christian Koeberl,[1]* Sharad Master,[2] Wolf U. Reimold[2]

The Neoproterozoic glaciations supposedly ended in a supergreenhouse environment, which led to rapid melting of the ice cover and precipitation of the so-called cap carbonates. If Earth was covered with ice, then extraterrestrial material would have accumulated on and within the ice and precipitated during rapid melting at the end of the glaciation. We found iridium (Ir) anomalies at the base of cap carbonates in three drill cores from the Eastern Congo craton. Our data confirm the presence of extended global Neoproterozoic glaciations and indicate that the duration of the Marinoan glacial episode was at least 3 million, and most likely 12 million, years.

The Snowball Earth hypothesis (*1*–*3*) states that the Sturtian [about 710 million years ago (Ma)] and Marinoan glaciations (about 635 Ma) were of global extent and lasted for several million years each. A variation of this hypothesis, called the Slushball Earth, requires milder conditions without substantial equatorial sea ice (*4*, *5*). The Snowball Earth glaciations would have ended abruptly in a greenhouse environment, whereas the Slushball would have experienced a slower deglaciation. Silicate weathering and photosynthesis, which are the major sinks for CO_2 at present, would have been inhibited by the ice that covered both continents and oceans, and huge amounts of CO_2 could have accumulated in the atmosphere. Greenhouse gases, particularly large amounts of CO_2 (up to ~0.12 bar), would have been needed to overcome the high albedo caused by the glaciation and would have caused rapid melting (*6*). This scenario has led to an estimate for the duration of a Snowball glaciation of ~4 million to 30 million years (My), under the assumption of a modern rate for CO_2 outgassing from subaerial volcanism, with no air-sea gas exchange, lower solar luminosity in the Neoproterozoic, and reduced pelagic deposition of carbonate to reduce the release of volcanic CO_2 at convergent margins (*7*). This estimate is in broad agreement with a >6- to >10-My duration derived from the $\delta^{13}C$ isotopic excursion in the Otavi (North Namibia) cap carbonates (*2*). Multiple magnetic polarity reversals within the Elatina Formation (South Australia) suggest a minimum time duration of several hundred thousand to 1 million years for the Marinoan glacial epoch (*8*).

If Earth was indeed covered by ice for long periods, extraterrestrial material would have accumulated on and within the ice and would have been precipitated at the base of the cap carbonates when the ice melted. To determine whether such an extraterrestrial signal is present at the base of the cap carbonates, we studied three drill cores that intersected diamictite/cap carbonate boundaries from the Lufilian tectonic arc in the Democratic Republic of the Congo and Zambia of the Eastern Congo craton (Fig. 1) (*9*).

We measured the concentrations of 43 elements by neutron activation analysis and x-ray fluorescence spectrometry, and we measured the Ir content by multiparameter coincidence spectrometry after neutron activation (*10*). Ir anomalies were found at the base of all cap carbonates after the Marinoan and Sturtian glaciations in the Nguba and Kundelungu Groups at Kipushi, as well as after the Sturtian glacial deposits in the Nguba Group at Chambishi. Ir and other platinum-group elements are typical proxies for extraterrestrial material, in which they are much more abundant than in Earth's upper mantle and crust. The average Ir concentration in cosmic matter is about 4.6×10^5 parts per thousand (ppt) (*11*), which is greater by a factor of about 10^4 than in crustal terrestrial rocks.

The accretion of extraterrestrial material during the Neoproterozoic is thought to have been dominated by the delivery of interplanetary dust particles (IDPs) over a time scale of millions of years (*12*). IDP accretion rates vary over periods ranging from a few thousand years (*13*) to millions of years (*14*). During glaciations, IDPs, as well as extraterrestrial matter from asteroids and comets that struck the Earth during that time (*9*), would have accumulated on the ice sheet.

Substantial Ir anomalies up to almost 2 parts per billion (ppb) mark the base of the cap carbonate deposits (Fig. 2) (*9*). Before ascribing an extraterrestrial origin to the Ir, possible terrestrial sources, including reduced sedimentation rates, increased meteor ablation rates, accretion of extraterrestrial material or of terrestrial dust (such as volcanic airborne particles), and anoxic conditions connected with sulfide precipitation in seawater need to be considered. Our geochemical data clearly indicate that the (substantial) Ir anomalies at the base of the cap carbonates are derived from extraterrestrial sources, whereas the other (smaller) Ir anomalies disappear or are greatly diminished when ratios with other elements are used [see (*9*) for detailed considerations]. Thus, these variations can be attributed to changing deposition rates or to the dissolution of an extraterrestrial signal caused by the addition of sediment.

Further confirmation that the Ir anomaly at the Kipushi Petit Conglomerat/cap carbonate transition (KPCCT) is of extraterrestrial origin comes from Cr/Ir and Au/Ir ratios of 2.9×10^3 and 0.11, respectively. These values are similar to those of C1 chondrites (carbonaceous chondrites type 1) (5.5×10^3 and 0.29, respectively) (*15*). Cr/Ir and Au/Ir ratios from other samples show higher values ranging from 8.4×10^4 to 1.8×10^6 and 1.1 to 80, respectively (Fig. 2).

In contrast to the sharp Ir anomaly at the KPCCT, the Nguba Group Ir anomaly extends over a broader interval, between 236.91 and 237.93 m, with a maximum of 648 ppt of Ir at 237.93 m. The integrated Ir concentrations are, however, as high as those at the other location. This Ir anomaly does not occur exactly at the Kipushi Grand Conglomerat/cap carbonate transition (KGCCT), but 0.63 m above, at 238.56 m in the cap carbonate succession (Fig. 2). Ir/element ratios with Fe, Cs, and Al, compared with the Grand Conglomerat and cap carbonate succession, are much higher in

[1]Department of Geological Sciences, University of Vienna, Althanstrasse 14, A-1090 Vienna, Austria. [2]Impact Cratering Research Group, School of Geosciences, University of the Witwatersrand, Private Bag 3, Johannesburg 2050, South Africa.

*To whom correspondence should be addressed. E-mail: christian.koeberl@univie.ac.at